2009 American Control Conference
Hyatt Regency Riverfront, St. Louis, MO, USA
June 10-12, 2009

Fractional Order Periodic Adaptive Learning Compensation for Cogging Effect in PMSM Position Servo System

Ying Luo†, YangQuan Chen‡, Hyo-Sung Ahn§, and Youguo Pi¶

Abstract— **Fractional calculus is a generalization of the integration and differentiation to the fractional (non-integer) order. In this paper, we devised a fractional-order periodic adaptive learning compensation (FO-PALC) method for cogging effect minimization for permanent magnetic synchronous motors (PMSM) position and velocity servo system. Cogging effect is a major disadvantage of PMSM. In fact, the cogging force in PMSM is a position-dependent periodic disturbance. In our FO-PALC scheme, in the first trajectory period, a fractional order adaptive compensator for cogging effect is designed to guarantee the boundedness of all signals. From the second repetitive trajectory period and onward, one period previously stored information along the state axis is used in the current adaptation law together with a fractional order low pass filter. Both stability analysis and experimental illustrations are presented to show the benefits from using fractional calculus in periodic adaptive learning compensation for cogging effects in PMSM servo systems.**

Index Terms— **Fractional calculus, cogging force, permanent magnet synchronous motor (PMSM), adaptive control, periodic adaptive learning control, state-dependent disturbance.**

I. Introduction

Fractional calculus is a generalization of the integration and differentiation to the fractional (non-integer) order. This conception of extending classical integer order calculus to non-integer order case has a firm and long-standing theoretical foundation. The interest of this subject has been known since of the development of the classical (integer-order) calculus, the first reference may be associated with the correspondence between Leibniz and L'Hospital in 1695 [1]. However, the fractional calculus concept was not widely applied into control engineering for hundreds of years, because of the unfamiliar idea and the realization limitation of fractional order, few application literatures were available at that time [2]. In the last several decades, as better understanding of the potential of fractional calculus, it is being accepted that fractional order calculus will be more and more useful in various sciences and engineering areas. For example, in motion control, a benchmark study on fractional order PID control of DC-motor with elastic shaft was presented in [3]. Some other example applications can be found in [4] [5] [6] [7].

In motion control areas, permanent magnet synchronous motor (PMSM) has received widespread acceptance in high performance industrial servo applications of accurate speed and position control with its many excellent features [8] [9]. However, as a major disadvantage of PMSM, the cogging effect degrades the servo control performance, especially in low-speed applications. Therefore, cogging effect minimization techniques have been proposed in, e.g., [10] [11] [12] [13]. The cogging force as a position-dependent periodic disturbance [14] can be well compensated by using the so-called learning control method [15] [16]. In our previous work [17], an adaptive learning compensator for compensating cogging and coulomb friction in permanent-magnet linear motors is designed and in [18], a periodic adaptive learning compensation (PALC) method is suggested for PMSM servo systems.

In the present paper, we devised a fractional-order periodic adaptive learning compensation (FO-PALC) method for cogging effect minimization in PMSM position and velocity servo system. In our FO-PALC scheme, in the first trajectory period, a fractional order adaptive compensator for cogging effect is designed to guarantee the boundedness of all signals. From the second repetitive trajectory period and onward, one period previously stored information along the state axis is used in the current adaptation law together with a fractional order low pass filter. Both stability analysis and numerical and experimental illustrations are presented to show the benefits from using fractional calculus in periodic adaptive learning compensation for cogging effects in PMSM servo systems.

The major contributions of this paper include: 1) A new fractional order periodic adaptive learning compensation for cogging effect; 2) Stability proof of the system with the proposed fractional order adaptive compensation method; 3) Experiment verification of FO-PALC for cogging-like disturbance on the real-time dynamometer position control system; 4) Demonstration of the advantage of the FO-PALC for cogging effect by performing the experimental comparisons with the traditional integer order PALC.

II. PMSM Position Servo System and Cogging Effect

A. PMSM Position Servo System Simulation Model

Under the assumption that the saturation, eddy currents and hysteresis losses are negligible in a permanent magnetic (PM) synchronous motor [19], the mechanical equations and electrical equations of a PMSM in the synchronous rotating reference frame are given by

$$\frac{\mathrm{d}\theta}{\mathrm{d}t} = \omega, \qquad \frac{\mathrm{d}\omega}{\mathrm{d}t} = \frac{1}{J}(T_m - T_l - B\omega), \tag{1}$$

$$\frac{\mathrm{d}i_d}{\mathrm{d}t} = \frac{1}{L_d}(V_d + \omega L_q i_q - R i_d - \omega\psi_{qm}), \tag{2}$$

$$\frac{\mathrm{d}i_q}{\mathrm{d}t} = \frac{1}{L_q}(V_q - \omega L_d i_d - R i_q - \omega\psi_{dm}), \tag{3}$$

where (1) represents the mechanical subsystem, and equations (2) and (3) represent the electrical subsystem. θ and ω are motor rotor angular position and speed, respectively; B is the friction coefficient; J is the moment of inertia of the rotor; T_m is the motor electromagnetic torque generated, and T_l is the load torque applied; i_d and i_q are stator currents along the d and q axes, respectively; V_d and V_q are the voltages along d and q axes, respectively; R is the stator resistance; L_d and L_q are the stator self-inductances in the d and q axes, respectively, it has been assumed that as the surface

†Email: ying.luo@ieee.org; Ying Luo is a Ph.D. candidate with the Department of Automation Science and Technology in South China University of Technology, Guangzhou, P.R. China and he was an exchange Ph.D. student at Center for Self-Organizing and Intelligent Systems (CSOIS), Dept. of Electrical and Computer Engineering, Utah State University, Logan, UT, USA from Sept. 2007 to Feb. 2009 under the full financial support from the China Scholarship Council (CSC).

‡Corresponding author, Email: yqchen@ieee.org; Tel. 01(435)797-0148; Fax: 01(435)797-3054; Electrical and Computer Engineering Dept., Utah State University, Logan, UT 84341, USA. URL: http://www.csois.usu.edu/people/yqchen.

§hyosung@gist.ac.kr; Dept. of Mechatronics, Gwangju Institute of Science and Technology (GIST), Gwangju, Korea.

¶auygpi@scut.edu.cn; Dept. of Automation Science and Technology, South China University of Technology, China.

mounted PMSM is non-salient, L_d and L_q are the same denoted by L.

Our simulation model of PMSM position servo system consists of three closed-loops for position, speed and current, respectively. More details about these three closed-loops, and the SVPWM algorithm are introduced in [18].

B. Cogging Effect

Cogging force is produced by the magnetic attraction between the rotor mounted permanent magnets and the stator [18]. It is the circumferential component of attractive force that attempts to maintain the alignment between the stator teeth and the permanent magnets. the cogging force spectrum depends only on the geometry and number of the stator slots, cogging force harmonics appear at frequencies that are multiple of the $N_{slot-pp}f_s$, where $N_{slot-pp}$ is the number of slots per pole pair and f_s is the electrical frequency of the rotor. Analytical modeling of the cogging force is changing since its production mechanism involves complex field distribution around state slots [20].

By using the concept of field oriented control of the PMSM, the d-axis current is controlled to be zero to maximize the output torque. Under this assumption, T_m is the motor electromagnetic torque, in the ideal case, is given by the following

$$T_m = K_t i_{qs} = \frac{3}{2}\frac{P}{2}\psi_{dm} i_q, \tag{4}$$

where K_t is the actually torque coefficient and P is the number of poles in the motor. However, in practice the motor torque can be expressed as

$$T_m = \frac{3}{2}\frac{P}{2}\psi_{dm} i_q + F_{cogging}, \tag{5}$$

where $F_{cogging}$ is the periodic torque pulsation due to cogging. In this paper, we also consider the cogging force as the general multi-harmonic form as considered in [18]

$$F_{cogging} = \sum_{i=1}^{\infty} A_i \sin(\omega_i x + \varphi_i). \tag{6}$$

where A_i is the amplitude, ω_i is the state-dependent cogging force frequency, and φ_i is the phase angle. In order to compensate the cogging force of general signal shape, it is suggested to make use of the periodicity of the position-dependent cogging disturbance.

III. Fractional Order Periodic Adaptive learning Compensation for Cogging Effect

A. Problem Formulation

In this section, a fractional order state-dependent periodic adaptive learning compensator for cogging is designed. The cogging force of (6) can be written as: $-a(\theta)$, where $a(\theta)$ is the function of θ. In this paper, to present our ideas clearly, without loss of generality, The motion control system is modeled as follows

$$\dot{\theta}(t) = v(t), \tag{7}$$

$$\dot{v}(t) = u - \frac{a(\theta)}{J} - T_{l'} - B_1 v, \tag{8}$$

$$u = \frac{1}{J}T_m, \quad T_{l'} = \frac{1}{J}T_l, \quad B_1 = \frac{B}{J}$$

where θ is the periodic rotor angle position; v is the velocity; u is the control input and $a(\theta)$ is the unknown position-dependent cogging disturbance which repeats every pole-pitch, at the same time $a(\theta)$ should be bounded and denoting

$$|a(\theta)| \le b_0, \quad \forall\theta. \tag{9}$$

In this section, to avoid text repetition yet to be as self-containing as possible, the notations not explained in the text can be found in [21].

Let us define

$$e_a(s(t)) = a(s(t)) - \hat{a}(s(t)), \tag{10}$$

where $\hat{a}(s(t)) = \hat{a}(t)$ (note: t is the current time corresponding to the current total passed trajectory $s(t)$). Here, let us change (10) into time-domain such as:

$$e_a(s(t)) = a(s(t)) - \hat{a}(s(t)) = a(t) - \hat{a}(t) = e_a(t). \tag{11}$$

In the same way, the following relationships are true:

$$v_d(s(t)) = v_d(t), \ v(s(t)) = v(t),$$

and the following notations are also defined

$$e_\theta(t) = \theta_d(t) - \theta(t), \ e_v(t) = v_d(t) - v(t). \tag{12}$$

The control objective is to track or servo the given desired position $\theta_d(t)$ and the corresponding desired velocity $v_d(t)$ with tracking errors as small as possible. In practice, it is reasonable to assume that $\theta_d(t)$ and $v_d(t)$ are both bounded signals.

The feedback controller is designed as:

$$u(t) = \dot{v}_d(t) + T_{l'} + \frac{\hat{a}(t)}{J} + \alpha m(t) + \gamma e_v(t), \tag{13}$$

with

$$m(t) := \gamma e_\theta(t) + e_v(t), \tag{14}$$

where α and γ are positive gains; $\hat{a}(t)$ is an estimated cogging force from an adaptation mechanism to be specified later; $\dot{v}_d(t)$ is the desired acceleration.

Our fractional order adaptive control law in the first trajectory period and the periodic adaptive learning control law after the first trajectory period are designed as follows:

$$\hat{a}(t) = \begin{cases} -\varepsilon_0 \frac{\mathrm{d}^\beta}{\mathrm{d}t^\beta}\hat{a}(t) + \delta\hat{a}_1(t) + \frac{K}{J}m_1(t) & \text{if} \quad s \ge s_p \\ z - \mu v & \text{if} \quad s < s_p \end{cases} \tag{15}$$

where

$$\hat{a}_1(t) =: \hat{a}(t - P_k),$$
$$m_1(t) =: m(t - P_k),$$

where $\varepsilon_0 \ge 0$, $\beta \in (0, 1]$ and $0 < \delta < 1$; P_k is the trajectory cycle and K is a positive design parameter called the periodic adaptation gain; μ is also a positive design parameter. In our analysis part, the following tuning mechanism is designed for z:

$${}_0D_t^\nu z(t) = \mu[\dot{v}_d(t) + \alpha m(t) + \gamma e_v(t)] + \frac{e_v(t)}{J}, \tag{16}$$

where

$$\nu \in (0, 1], \quad z(t)|_{t=0} = 0.$$

In this paper, the following Caputo definition for fractional derivative is used, which allows utilization of initial values of classical integer-order derivatives with known physical interpretations [22]

$$\frac{\mathrm{d}^\alpha f(t)}{\mathrm{d}t^\alpha} = \frac{1}{\Gamma(\alpha - n)}\int_0^t \frac{f^{(n)}(\tau)\mathrm{d}\tau}{(t-\tau)^{\alpha+1-n}}, \tag{17}$$

where n is an integer satisfying $n - 1 < \alpha \le n$.

Remark 3.1: If $\nu \in (0, 1)$ or $\varepsilon_0 > 0$ and $\beta \ne 1$, our designed control law (15) is the new fractional order periodic adaptive learning compensation scheme; if $\nu = 1$ and $\varepsilon_0 = 0$, our designed control law (15) is the integer order PALC scheme [21]. The main purpose of this paper is to illustrate how the non-integers α and ν can benefit the learning controller.

B. Stability Analysis

Now, based on the above discussions, the following stability analysis of the proposed fractional order adaptive compensation method in the first period and the periodic adaptive learning compensation scheme after the first period are presented respectively. Our fractional order periodic adaptive learning compensation approach is summarized as follows:

- When $s(t)<s_p$, the system under fractional order adaptive control is bounded input bounded output.
- When $s(t)\geq s_p$, the system is stabilized to follow the desired speed at the desired position. By trajectory periodic adaptation, the unknown cogging is estimated.

Consider two cases: 1) when $0 \leq t < P_1$ $(0 \leq s < s_p)$ and 2) when $t \geq P_1$ $(s \geq s_p)$. The key idea is that, for case 1), it is required to show the finite time boundedness of all signals; for case 2), it is necessary to show the asymptotic stability of equilibrium points.

First, let us consider the case 1) when $t < P_1$ $(s < s_p)$.

If choosing $\nu = 1$, the control law $\hat{a} = z - \mu v$ in (15) is the integer order adaptive control scheme. We have the theorem below.

Theorem 3.1: If $|\partial a(\theta)/\partial\theta| < b_a$ (bound of changes in $a(\theta)$), $\mu > \frac{1}{4}J(1 + b_a^2)$ and $(\alpha + \gamma) > 1$, the equilibrium points of $e_\theta(t)$ and $e_v(t)$ are bounded, when $t < P_1$ $(s < s_p)$.

For a proof of Theorem 3.1, see [21].

If choosing $0 < \nu < 1$, the control law $\hat{a} = z - \mu v$ in (15) is the new fractional order adaptive compensation scheme.

Firstly, the following lemma is needed for the proof of Theorem 3.2.

Lemma 3.1: An ordinary input/output relation (with only integer derivatives) can be written in a polynomial representation

$$\begin{aligned} P(\sigma)\xi &= Q(\sigma)u, \\ y &= R(\sigma)\xi. \end{aligned} \tag{18}$$

where $u \in \Re^{\bar{m}}$ is the control signal, $\xi \in \Re^{\bar{n}}$ is the intermediate signal, and the $y \in \Re^{\bar{p}}$ is the output signal; P, Q, R are polynomial matrices in the variable σ of dimensions $\bar{n} \times \bar{n}$, $\bar{n} \times \bar{m}$ and $\bar{p} \times \bar{n}$ respectively; σ can be seen either as the symbol for the usual derivative d^ν or s^ν, the complex function in Laplace variable s, when all initial conditions are zero.

If the triplet (P, Q, R) of polynomial matrices is minimal, we have the equivalence: system (18) is bounded-input bounded-output iff $\det(P(\sigma)) \neq 0$ $\forall\sigma$ with $|\arg(\sigma)| < \nu\frac{\pi}{2}$.

For a proof of Lemma 3.1, see [23].

Theorem 3.2: If choosing proper parameters α, γ and μ to ensure

$$|\arg(w_i)| > \nu\frac{\pi}{2},$$

where w_i are the solutions of equation (19),

$$w^{2pq+p^2} + aw^{pq+p^2} + bw^{pq} + dw^{p^2} + c = 0, \tag{19}$$

where $\nu = p/q$, p and q are integers,

$$\begin{aligned} a &= \alpha + \gamma + \frac{1}{J}\mu + B_1, \\ b &= \frac{1}{J}\mu(\alpha + \gamma) + \frac{1}{J^2}, \\ c &= \frac{1}{J}\mu\alpha\gamma, \\ d &= \alpha\gamma. \end{aligned}$$

then $e_\theta(t)$ and $e_v(t)$ are bounded, when $t < P_1$ $(s < s_p)$.

For a proof of Theorem 3.2, see [21].

Now, let us investigate the case 2) when $t \geq P_1$ $(s \geq s_p)$. We have the following stability result:

Theorem 3.3: When $t \geq P_1$ $(s \geq s_p)$, the control law (13) and the periodic adaptation law (15) guarantee that $e_\theta(t)$, $e_v(t)$ and $e_a(t)$ all approach 0 as $t \to \infty$ $(s \to \infty)$.

To simplify the presentation of our proof, let us make the following notation:

$$\eta_i(t) = \eta(t - \sum_{j=1}^{i} P_{k+1-j}), \quad i = 1, 2, ..., N,$$
$$\eta \in \{\theta_d, \theta, v_d, v, a, \hat{a}, e_\theta, e_v, e_a, m, S\}.$$

Proof: First of all, to avoid confusion in the beginning, let us first consider the integer order case by setting $\varepsilon_0 = 0$ in (15).

From now on, denoting $t' = t - P_1$. So, when $t = P_1$, $t' = 0$.

From (8) and (13),

$$\begin{aligned} \dot{v}(t') &= \dot{v}_d(t') + T_{l'} + \frac{1}{J}\hat{a}(t') + (\alpha + \gamma)e_v(t') \\ &\quad + \alpha\gamma e_\theta(t') - \frac{1}{J}a(t') - T_{l'} - B_1(v_d(t') - e_v(t')) \\ &= \dot{v}_d(t') + \frac{1}{J}\hat{a}(t') + \alpha\gamma e_\theta(t') + (\alpha + \gamma)e_v(t') \\ &\quad - \frac{1}{J}a(t') - B_1(v_d(t') - e_v(t')), \end{aligned} \tag{20}$$

and from (12),

$$\begin{aligned} \dot{e}_v &= \dot{v}_d(t') - \dot{v}(t') \\ &= -\alpha\gamma e_\theta(t') - (\alpha + \gamma + B_1)e_v(t') \\ &\quad + \frac{1}{J}a(t') - \frac{1}{J}\hat{a}(t') + B_1 v_d(t'). \end{aligned} \tag{21}$$

Then, from (7),

$$\begin{aligned} \dot{e}_\theta &= \dot{\theta}_d(t') - \dot{\theta}(t') \\ &= v_d(t') - v(t') \\ &= e_v(t'), \end{aligned} \tag{22}$$

and substituting (22) into (21) yields

$$\begin{aligned} \ddot{e}_\theta(t') &= -\alpha\gamma e_\theta(t') - (\alpha + \gamma + B_1)\dot{e}_\theta(t') \\ &\quad + \frac{1}{J}a(t') - \frac{1}{J}\hat{a}(t') + B_1 v_d(t'). \end{aligned} \tag{23}$$

So, we have

$$\begin{aligned} &\ddot{e}_\theta(t') + (\alpha + \gamma + B_1)\dot{e}_\theta(t') + \alpha\gamma e_\theta(t') \\ &= \frac{1}{J}a(t') - \frac{1}{J}\hat{a}(t') + B_1 v_d(t'). \end{aligned} \tag{24}$$

From Theorem 3.1, when $t = P_1$, $e_\theta(t')$ and $e_v(t')$ are bounded and denoting

$$e_\theta(t')|_{t=P_1} = e_\theta(t')|_{t'=0} \leq b_\theta, \tag{25}$$

$$\dot{e}_\theta(t')|_{t=P_1} = e_v(t')|_{t=P_1} = e_v(t')|_{t'=0} \leq b_v, \tag{26}$$

$$\hat{a}(t')|_{t=P_1} = \hat{a}(t')|_{t'=0} \leq b_{\hat{a}}. \tag{27}$$

Performing the Laplace transform of (24) with operator s' leads to

$$\begin{aligned} &s'^2 E_\theta(s') + (\alpha + \gamma + B_1)s' E_\theta(s') + \alpha\gamma E_\theta(s') \\ &= F(s') - \frac{1}{J}\hat{A}(s') + e_v(t')|_{t'=0} \\ &\quad + (s' + \alpha + \gamma + B_1)e_\theta(t')|_{t'=0}, \end{aligned} \tag{28}$$

where

$$\begin{aligned} F(s') &= L\{f(t')\} \\ &= L\{\frac{1}{J}a(t') + B_1 v_d(t')\}, \end{aligned} \tag{29}$$

$$\hat{A}(s') = L\{\hat{a}(t')\}, \tag{30}$$

From our adaptation law (15) as $s \geq s_p$, and

$$\begin{aligned} m_1(t) &= \gamma e_\theta(t-P_k) + e_v(t-P_k), \quad (31) \\ e_\theta(t)|_{t=0} &= \theta_d(t)|_{t=0} - \theta(t)|_{t=0} = 0, \quad (32) \end{aligned}$$

so we can obtain the Laplace transforms

$$\begin{aligned} L\{e_\theta(t-P_k)\} &= e^{-P_k s'} E_\theta(s'), \quad (33) \\ L\{e_v(t-P_k)\} &= L\{\dot{e}_\theta(t-P_k)\} \\ &= (s' E_\theta(s') - e_\theta(t)|_{t=0}) e^{-P_k s'} \\ &= s' E_\theta(s') e^{-P_k s'}, \quad (34) \end{aligned}$$

then we have

$$\begin{aligned} \hat{A}(s') &= L\{\hat{a}(t')\} \\ &= \delta e^{-P_k s'} \hat{A}(s') + \frac{K}{J} e^{-P_k s'} (\gamma E_\theta(s') + s' E_\theta(s')), \end{aligned} \quad (35)$$

we have

$$\hat{A}(s') = \frac{\frac{K}{J}(s'+\gamma) e^{-P_k s'}}{1 - \delta e^{-P_k s'}} E_\theta(s'). \quad (36)$$

Then from (28) and (36), we can get

$$\begin{aligned} G(s') &= \frac{E_\theta(s')}{H(s')} \\ &= \frac{1}{s'^2 + as' + b + \frac{\frac{K}{J^2}(s'+\gamma)e^{-P_k s'}}{1-\delta e^{-P_k s'}}} \\ &= \frac{1 - \delta e^{-P_k s'}}{(1-\delta e^{-P_k s'})(s'^2 + as' + b) + \frac{K}{J^2}(s'+\gamma) e^{-P_k s'}} \\ &= \frac{\frac{1}{s'^2+as'+b}(1-\delta e^{-P_k s'})}{1 - [1 - \frac{\frac{K}{J^2}(s'+\gamma)}{s'^2+as'+b}] e^{-P_k s'}}, \quad (37) \end{aligned}$$

where

$$\begin{aligned} H(s') &= F(s') + e_v(t')|_{t'=0} \\ &\quad + (s' + \alpha + \gamma + B_1) e_\theta(t')|_{t'=0}, \quad (38) \\ a &= \alpha + \gamma + B_1, \\ b &= \alpha\gamma. \end{aligned}$$

Equation (37) can be treated as the transfer function of the system in Fig. 1. Once the equivalence has been shown, in order to guarantee the stability of the system (37), one must establish under which conditions each block in Fig. 1 is stable. The first block is $\frac{1}{s'^2+as'+b}$, which should be stable if all its characteristic roots have negative real parts. The second block is nothing more than a time delay, so it is always stable. Finally, the third block can be described as a positive-feedback closed-loop system with the term $(1 - \frac{\frac{K}{J^2}(s'+\gamma)}{s'^2+as'+b}) e^{-P_k s'}$ in the feedback path.

According to the Small Gain Theorem, the sufficient condition for the stability of the system (37) can be split into two conditions.

First stability condition:

$$\Re(\lambda) < 0, \quad \forall \lambda \in \{\lambda_i | \lambda_i^2 + a\lambda_i + b = 0\}. \quad (39)$$

Second stability condition:

$$|1 - \frac{\frac{K}{J^2}(s'+\gamma)}{s'^2 + as' + b}|_{s'=j\omega} < 1, \quad \forall \omega. \quad (40)$$

These two stability conditions are easy to satisfy when designing the proposed learning control systems. There exists a choice of K, γ, a and b which can satisfy the second stability condition (40). For example, when $\omega = 0$, $|1 - \frac{K\gamma/J^2}{b}| < 1$. From Theorem 3.1, Theorem 3.2, and equations (9) (29), the input signal $f(t')$ in system (37) is bounded. So, under the above two stability conditions, the output signal $e_\theta(t')$ in system (37) is also bounded. In order to establish $e_\theta(t') = 0$ as $t \to \infty$, let us apply the Final Value Theorem with the condition $H(0) \neq \infty$ from (38),

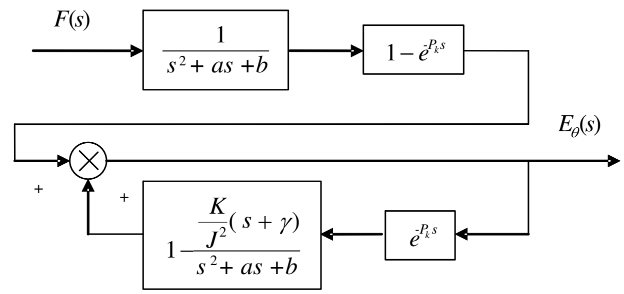

Fig. 1. Alternative block diagram for the closed-loop control system (37)

$$\lim_{t\to\infty} e_\theta(t') = \lim_{s'\to 0} s' H(s') G(s') = 0. \quad (41)$$

where we used the obvious fact that $G(0) = 0$ in (37).

Now, let us turn to the case when $\varepsilon_0 > 0$ in (15). In this case, then, equation (37) becomes

$$\begin{aligned} G(s') &= \frac{E_\theta(s')}{H(s')} \\ &= \frac{\frac{1}{s'^2+as'+b}(1 - \delta e^{-P_k s'} + \varepsilon_0 s'^\beta)}{1 - [1 - \frac{\frac{K}{J^2}(s'+\gamma)}{s'^2+as'+b} - \frac{\varepsilon_0 s'^\beta}{e^{-P_k s'}}] e^{-P_k s'}}. \quad (42) \end{aligned}$$

where

$$\begin{aligned} H(s') &= F(s') + (s' + \alpha + \gamma + B_1) e_\theta(t')|_{t'=0} \\ &\quad + e_v(t')|_{t'=0} + \frac{\varepsilon_0 \hat{a}(t')|_{t'=0}}{1 - \delta e^{-P_k s'} + \varepsilon_0 s'^\beta}. \quad (43) \end{aligned}$$

Following the same reasoning shown in the case of $\varepsilon_0 = 0$, we can similarly conclude that $e_\theta(t') = 0$ as $t \to \infty$.

Remark 3.2: ε_0 and β in (15) can be perceived as a fractional order low pass filter $\frac{1}{1+\varepsilon_0 s'^\beta}$. This will offer potential benefits in achieving better performance in the periodic learning control in terms of "long-term stability" as addressed in [24] where an integer order first order low-pass filter is proposed under the term of "dynamic PALC."

Finally, from (22), we have

$$E_v(s') = s' E_\theta(s') - e_\theta(t')|_{t'=0} = s' G(s') H(s') - e_\theta(t')|_{t'=0}. \quad (44)$$

So, similarly, as $e_\theta(t')|_{t'=0}$ is finite, we can conclude from (44) that the error signal $e_v(t')$ also approaches 0 as $t \to \infty$ since

$$e_v(\infty) = \lim_{s'\to 0} s' E_v(s') = 0.$$

■

IV. Experiments

A. Introduction to the Experiment Platform

A fractional horsepower dynamometer was developed as a general purpose experiment platform to emulate mechanical nonlinearities such as frictions, state-dependent disturbances, etc. This lab system can be used as a research platform to test various advantage control schemes [25].

The architecture of the dynamometer control system is shown in Fig. 2. The Dynamometer includes the DC motor to be tested,

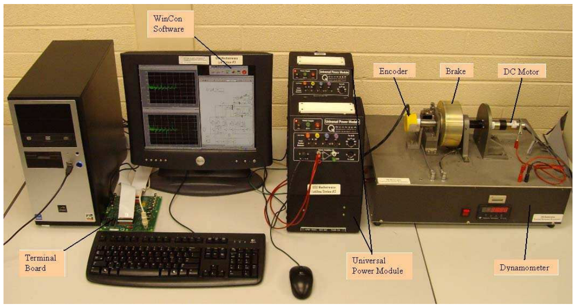

Fig. 2. The dynamometer setup used in PALC experiments

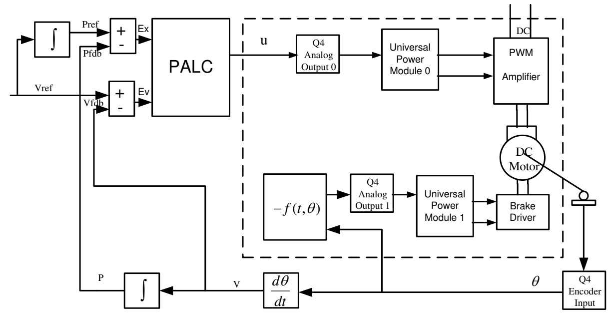

Fig. 3. Block diagram of the cogging-like disturbance PALC in the Dynamometer position control system

a hysteresis brake for applying load to the motor, a load cell to provide force feedback, an optical encoder for position feedback and a tachometer for velocity feedback. The dynamometer was modified to connect to a Quanser MultiQ4 terminal board in order to control the system through Matlab/Simulink Real-Time Workshop (RTW) based software. This terminal board connects with the Quanser MultiQ4 data acquisition card. Then, using the Matlab/Simulink environment, which uses the WinCon application, from Quanser, to communicate with the data acquisition card. This brings rapid prototyping and experimental platform.

Without loss of generality, consider a servo control system modeled by:

$$\dot{x}(t') = v(t'), \tag{45}$$

$$\dot{v}(t') = u(t') - f(t,x) - \frac{B_d}{J_d}v. \tag{46}$$

where x is the position or displacement, v is the velocity, $f(t,x)$ is the unknown disturbance, which may be state-dependent or time-dependent, B_d and J_d are the frictional coefficient and moment of inertia of the dynamometer respectively, and u is the control input. The system under consideration, i.e. the DC motor in the dynamometer, has a transfer function $1.52/(1.01s+1)$. Moreover, the presence of the hysteresis brake allows us to add a time-dependent or statedependent disturbance (load) to the motor. These factors combined can emulate a system similar to the one given by (45) and (46). A controller can be designed for such a problem and can be tested in the presence of the real disturbance as introduced through the hysteresis brake.

B. Experiments on the Dynamometer

The proposed method is verified on the real-time dynamometer position control system. The hysteresis brake force is designed as multi-harmonics cogging-like disturbance

$$f(t,x) = \frac{T_d}{J_d} + \frac{a(t')}{J_d} = \frac{T_d}{J_d} + F_{diturbance}, \tag{47}$$

where

$$\frac{T_d}{J_d} = 1,$$
$$F_{diturbance} = 10\cos(x) + 5\cos(2x) + 2.5\cos(3x).$$

when x is replaced by θ, then the system (45) and (46) is the same format with (7) and (8). As mentioned in [18], after using vector control (control i_d to 0), it will make the nonlinear and coupling characteristics of PMSM become decoupled. Thus, the torque magnitude control of PMSM is only need to control the current in the direction of q-axis, thus we can control a PMSM as easy as to control a DC motor. So, we can testify the periodic adaptive learning compensation methods for cogging effect on the dynamometer platform, Fig. 3 shows the block diagram. The control gains in (13) and (15) were selected as: $\alpha = 20$, $\gamma = 10$ and $\mu = 0.5$, the periodic adaptation gain K was selected as 0.01, and δ is also chosen as 1 in (15).

As an illustration, two experimental cases are performed.

- Case-1e: Integer order periodic adaptive learning compensation for cogging-like disturbance;
- Case-2e: Fractional order periodic adaptive learning compensation for cogging-like disturbance;

In both of the two experimental cases, the following reference trajectory and velocity signals are used:

$$s_d(t') = 5t\ (rad),$$
$$v_d(t') = 5\ \ (rad/s).$$

Case-1e: Integer order periodic adaptive learning compensation for cogging-like disturbance: For this case, choosing $\nu = 1$ in adaptive law (15) as integer order PALC for cogging-like effect.

Figures 5(a) and 5(b) show the position/speed tracking errors using integer order periodic adaptive learning compensation method. We can observe that, the integer order periodic adaptive learning compensation method works efficiently comparing with the tracking errors without compensation in Figures 4(a) and 4(b).

Case-2e: Fractional order periodic adaptive learning compensation for cogging-like disturbance: For this case of experimental test, choosing $\nu = 0.5$ in adaptive law (15), fractional order PALC is used for cogging-like effect. Figures 6(a) and 6(b) show the position/speed tracking errors using fractional order periodic adaptive learning compensation method. Comparing with figures 5(a) and 5(b), we can clearly observe that the performance of using fractional order periodic adaptive learning compensation method is much better than that of using integer order periodic adaptive learning compensation method for cogging-like disturbance in real-time position control platform.

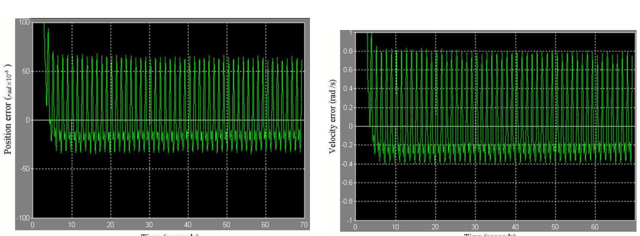

(a) Position (b) Velocity

Fig. 4. Experiment. Tracking errors without compensation.

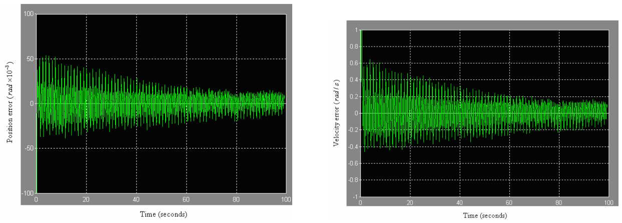

(a) Position (b) Velocity

Fig. 5. Experiment. Tracking errors with integer order periodic adaptive learning compensation.

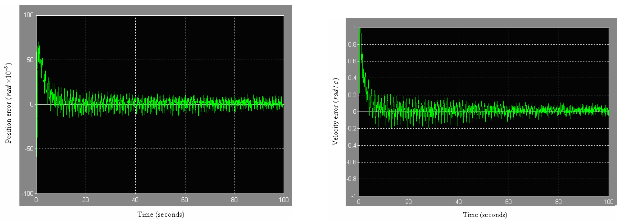

(a) Position (b) Velocity

Fig. 6. Experiment. Tracking errors with fractional order periodic adaptive learning compensation.

Note again that, the final version of this paper will include the case of fractional order low pass filter in the PALC scheme for better maintaining the long-term stability.

V. Conclusion

In this paper, a new fractional order periodic adaptive learning compensation method is proposed to compensate the cogging effect in PMSM position and velocity servo system. In our FO-PALC scheme, in the first trajectory period, a fractional order adaptive compensator for cogging effect is designed to guarantee the boundedness of all signals. From the second repetitive trajectory period and onward, one period previously stored information along the state axis is used in the current adaptation law together with a fractional order low pass filter. Both stability analysis and experimental illustrations are presented to show the benefits from using fractional calculus in periodic adaptive learning compensation for cogging effects in PMSM servo systems. We believe, the basic ideas of using fractional calculus in this paper are applicable to iterative learning control as well as repetitive control.

Acknowledgement

Ying Luo would like to thank to Dr. Huifang Dou for her expertise in cogging compensation of PMLM (permanent magnet linear motor) and to the China Scholarship Council (CSC) for the financial support.

References

[1] K. B. Oldham and J. Spanier, "The fractional calculus," Academic Press, New York and London, 1974.

[2] M. Axtell and M. E. Bise, "Fractional calculus applications in control systems," in *Proc. IEEE nat. aerospace and electronics conference*, New York, USA, 1990, pp. 563–566.

[3] D. Y. Xue, C. N. Zhao, and Y. Q. Chen, "Fractional order PID control of a DC-motor with elastic shaft; a case study," in *Proc. of American Control Conference*, MN, USA, June 2006.

[4] Dingyu Xue and YangQuan Chen, "Fractional order calculus and its applications in mechatronic system controls organizers," in *Proceedings of the 2006 IEEE International Conference on Mechatronics and Automation*, June 2006, p. 33.

[5] Vinagre B. M., Petras I., Podlubny I., and Chen Y. Q., "Using fractional order adjustment rules and fractional order reference models in model reference adaptive control," *Nonlinear Dynam*, vol. 29, pp. 269–279, 2002.

[6] Ladaci S. and Charef A., "On fractional adaptive control," *Nonlinear Dynam*, vol. 43, no. 4, pp. 365–378, 2006.

[7] Ladaci S. and Charef A., "An adaptive fractional PID controller," in *Proceedings TMCE 2006 international symposium series on tools and methods of competitive engineering*, Ljubljana, Slovenia, April 1822 2006, pp. 1533–1540.

[8] M. A. Rahman and M. A. Hoque, "On-line adaptive artificial neural network based vector control of permanent magnet synchronous motor," *IEEE Trans. Energy Convers.*, vol. 13, no. 4, pp. 311–318, 1998.

[9] Y. Zhang, C. M. Akujuobi, W. H. Ali, C. L. Tolliver, and L.-S. Shieh, "Load disturbance resistance speed controller design for PMSM," *IEEE Trans. Ind. Electron.*, vol. 53, no. 4, pp. 1198–1208, 2006.

[10] T. M. Jahns and W. L. Soong, "Pulsating torque minimization techniques for permanent-magnet ac motor drives - a review," *IEEE Trans. Ind. Electron.*, vol. 43, no. 2, pp. 321–330, 1996.

[11] C. Chan, J. Jiang, G. Chen, X. Wang, and K. Chau, "A novel polyphase multipole square-wave permanent magnet motor drive for electric vehicles," *IEEE Trans. Ind. Appl.*, vol. 30, no. 5, pp. 1258–1266, 1994.

[12] P. J. Hor, Z. Q. Zhu, D. Howe, and J. Rees-Jones, "Minimization of cogging force in a linear permanent magnet motor," *IEEE Trans. on Magnetics*, vol. 34, no. 5, pp. 3544–3547, 1998.

[13] D. C. Hanselman, "Minimum torque ripple, maximum efficiency excitation of brushless permanent magnet motors," *IEEE Trans. on Ind. Electron.*, vol. 41, pp. 292–300, 1994.

[14] P. J. Hor, Z. Q. Zhu, D. Howe, and J. Rees-Jones, "Minimization of cogging force in a linear permanent-magnet motor," *IEEE Trans. on Magnetics*, vol. 34, no. 5, pp. 3544–3547, 1998.

[15] K. K. Tan, S. N. Huang, and T. H. Lee, "Robust adaptive numerical compensation for friction and force ripple in permanent-magnet linear motors," *IEEE Trans. on Magnetics*, vol. 38, no. 1, pp. 221–228, 2002.

[16] J.-X. Xu, S. K. Pands, Y.-J. Pan, and T. H. Lee, "A modular control scheme for PMSM speed control with pulsating torque minimization," *IEEE Trans. on Ind. Electron.*, vol. 51, pp. 526–536, 2004.

[17] Hyo-Sung Ahn, YangQuan Chen, and Huifang Dou, "State-periodic adaptive compensation of cogging and coulomb friction in permanent-magnet linear motors," *IEEE Transactions on Magnetics*, vol. 41, no. 1, pp. 90–98, 2005.

[18] Ying Luo, YangQuan Chen, and YouGuo Pi, "Authentic simulation studies of periodic adaptive learning compensation of cogging effect in PMSM position servo system," in *Proceedings of the Chinese Conference on Decision and Control (CCDC08)*, Yantai, Shandong, China, 2-4 July 2008, pp. 4760–4765.

[19] P. C. Krause, "Analysis of Electric Machinery," New York, McGraw-Hill, 1987.

[20] V. Petrovic, R. Ortega, A. M. Stankovic, and G. Tadmor, "Design and implementation of an adaptive controller for torque ripple minimization in PM synchronous motors," *IEEE Trans. on Power Electron.*, vol. 15, pp. 871–880, 2000.

[21] Ying Luo, YangQuan Chen, Hyo-Sung Ahn, and YouGuo Pi, "A high order periodic adaptive learning compensator for cogging effect in PMSM position servo system," *IEEE Trans. on Magnetics (submitted)*.

[22] I. Podlubny, "Fractional Differential Equations," Academic press, 1999.

[23] D. Matignon, "Stability results for fractional differential equations with applications to control processing," in *Computational engineering in systems applications*, Lille, France, July 1996, pp. 963–968.

[24] Ying Luo, YangQuan Chen, Hyo-Sung Ahn, and Youguo Pi, "Design of dual-high-order dynamic periodic adaptive learning controller for long-term cogging effect compensation," in *Proceedings of the 10th International Conference on Control, Automation, Robotics and Vision (ICARCV08) (accepted)*, Hanoi, Vietnam, December 2008.

[25] Y. Tarte, YangQuan Chen, Wei Ren, and K. Moore, "Fractional horsepower dynamometer - a general purpose hardware-in-the-loop real-time simulation platform for nonlinear control research and education," in *IEEE Conference on Decision and Control*, 13-15 Dec. 2006, pp. 3912–3917.